

## 2,3,5-Metallotriazoles: Amphoteric Mesoionic Chelates from Nitrosoguanidines

Mimi Simmons, Kayla Cummings Premack, E. Danae Guerra, Maeve J. Bohle, Kristopher A. Rosadiuk, and D. Scott Bohle\*

**Cite This:** *Inorg. Chem.* 2021, 60, 9621–9630

**Read Online**

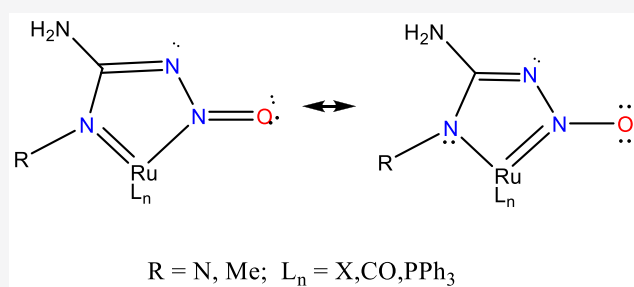
ACCESS |

Metrics & More

Article Recommendations

Supporting Information

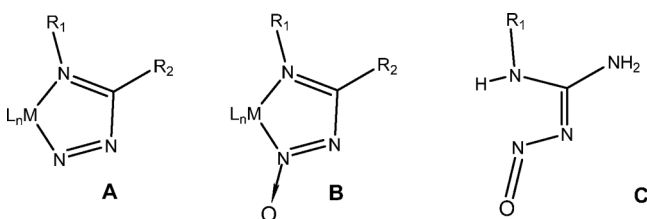
**ABSTRACT:** Soluble nitrosoguanidine- and *N*-methylnitrosoguanidine-based metallotriazole complexes of ruthenium(II) monocarbonyls have been prepared and characterized. Both nitrosoguanidines prove to be strong chelates with the formally  $\pi$ -accepting nitroso nitrogen binding *cis* to carbon monoxide and a  $\pi$ -donating amide *trans* to the CO. The resulting ensemble consists of ruthenium examples of 1-metallo-2,3,5-triazoles. The ruthenium coordination sphere is completed by anions, either  $\text{H}^-$ ,  $\text{Cl}^-$ , or  $\text{Ph}^-$ , *trans* to the nitroso group as well as two mutually *trans*  $\text{PPh}_3$  groups. The  $\pi$ -donating amide group is formally  $\text{sp}^2$  hybridized with a planar nitrogen to give a strongly bound five-membered chelating anion. Together, these results illustrate the remarkable



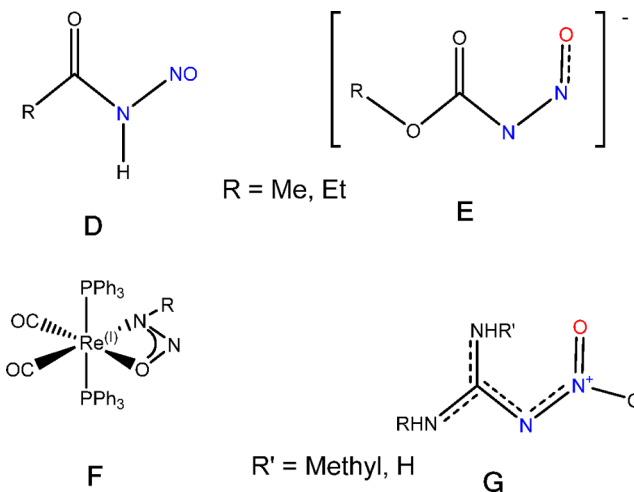
potential for the nitrosoguanidines as a family of new metal chelates.

### INTRODUCTION

1-Metallo-2,3,5-triazoles<sup>1–13</sup> (A) and their 2-*N*-oxides<sup>10–18</sup> (B) are members of a surprisingly small family of metallo-heterocycles with multiple bonds and delocalized bonding within the five-membered ring. In part, this scarcity is due to the limited synthetic pathways to these complexes, but an upsurge in interest in this class stems from recent studies that suggest new bonding,<sup>17</sup> cytotoxic,<sup>19</sup> and structural characteristics<sup>20</sup> for A and B.



Although the first members of this class ( $\text{R}_2 = \text{Ph}$ ,  $\text{R}_1 = \text{H}$ ) were structurally characterized in the products of oxidation of benzamidooximate and by trapping the resulting  $[\text{PhC}(\text{NH})(\text{NNO})]^-$  ligand in a diamagnetic  $\text{Ni}(\text{II})$  complex,<sup>18</sup> complexes like B were first described<sup>21</sup> in 1893 in the pioneering work of Joachim Thiele. In the course of characterizing the free *N*-oxide derivatives of B ( $\text{R}_2 = \text{NH}_2$ ,  $\text{R}_1 = \text{H}$ ), Thiele prepared B by coordinating the reduction product of nitroguanidine, nitrosoguanidine,  $(\text{H}_2\text{N})_2\text{CNNO}$  (C). More than a century later these original formulations were crystallographically confirmed<sup>14,15</sup> and then extended to other first-row complexes.<sup>15</sup> More recent approaches to this class include the

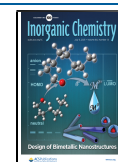


coordination of 2-diazoazines<sup>2,5,12,13</sup> and the metal-templated condensation of dialkylcyanamides and acetamidoximes.<sup>17,18,20,22</sup>

Our interest in this class stems from our recent work on the primary nitrosamides (D) that are frequently invoked

**Received:** March 21, 2021

**Published:** June 23, 2021



intermediates in the nitration of amines and the reduction of nitrosamides. Although as a class the nitrosamides are potent mutagenic carcinogens, few have been studied in depth and only a handful are known as discrete isolable materials. Perhaps the best understood set of derivatives, the nitrosocarbamates (**E**), was first described by Joachim Thiele in 1898.<sup>23</sup> In contrast with their scant chemistry<sup>24–26</sup> since Thiele's pioneering work, the biological interest in this class is burgeoning.<sup>27,28</sup> We recently demonstrated some of their potential by isolating and characterizing the first nitrosocarbamides complexes (**F**).<sup>29,30</sup> Among the unusual hydrolysis and degradation products of **F** is the release of nitrous oxide, which is attributed to the intermediacy of nitroxyl anions, NO<sup>-</sup>. As stable nitrosamides make up a small class of reagents, and because we sought to extend this potentially useful chemistry as a source of nitroxyl anions, we are exploring related compounds with carbamate-like character. The nitrosoguanidines (**C**) are excellent analogues and have hints of an equally unusual chemistry being dispersed in their rare literature.<sup>21</sup> Although the nitroguanidines (**G**) have a renowned chemistry<sup>31</sup> that includes high-energy applications of nitroguanidine itself,<sup>32</sup> their known<sup>33</sup> reduction to the corresponding nitrosoguanidines (**C**, **1a**) is seldom exploited, and thus, they have a limited chemistry.<sup>14,15,21</sup> The key problems that emerge from their known chemistry are the limited synthetic access to the nitrosoguanidines, their low solubility, and poor stability. We report herein solutions to these problems: (1) optimized syntheses of nitrosoguanidine and *N*-methyl-nitrosoguanidine (**1a** and **1b**) along with their structural, spectroscopic, and coordination properties, (2) a density functional theory (DFT) study of their metal binding properties and for the conformational dynamics and interconversion barriers for **1b**, (3) preparation of six ruthenium nitrosoguanidine complexes of **1a** and **1b** along with their crystal structures and spectroscopy, and (4) incorporation of a single *N*-methyl group on *N'* in **1b** that is sufficient to surmount many of the solubility issues found for **1a** and its complexes and suggests that the substituted nitrosoguanidine may have a rich unexplored chemistry. Taken together, these results suggest that the nitrosoguanidines are excellent chelating bidentate anionic ligands with a potentially rich coordination chemistry.

## EXPERIMENTAL SECTION

Starting materials were purchased or in the case of RuHCl(CO)(PPh<sub>3</sub>)<sub>3</sub>,<sup>34</sup> RuPhCl(CO)(PPh<sub>3</sub>)<sub>2</sub>,<sup>35,36</sup> and [RuH(NCCCH<sub>3</sub>)<sub>2</sub>(CO)(PPh<sub>3</sub>)<sub>2</sub>]ClO<sub>4</sub><sup>37</sup> prepared by literature methods. Infrared (IR) spectra were measured on a Bomem MB3000 FTIR spectrometer as KBr pellets, and <sup>1</sup>H and <sup>31</sup>P(<sup>1</sup>H) nuclear magnetic resonance (NMR) spectra were measured on a Bruker AVIIIHD 500 spectrometer at 22 °C and 500 MHz for <sup>1</sup>H, 202 MHz for <sup>31</sup>P, and 125 MHz for <sup>13</sup>C.

**Preparation of Nitrosoguanidine Derivatives.** Literature methods for the preparation of nitrosoguanidine and *N*-methyl-nitrosoguanidine were modified to improve the yield and purity of the final reagents. Both of the following methods employ and/or improve upon the zinc reduction of the corresponding nitroguanidines. Full characterization details are given here for the sake of completeness and to update the data for this family of derivatives with contemporary spectroscopic methods.

**Nitrosoguanidine.** Nitroguanidine (1.03 g, 0.01 mol) and 1.07 g of ammonium chloride are dissolved in 10 mL of dimethyl sulfoxide (DMSO) with stirring and cooled to near 10 °C with an ice/salt bath. Finely divided zinc (0.644 g, 1.1 equiv) is slowly added in portions over the course of 1 h, ensuring the solution does not warm suddenly at any stage during the addition. After the addition is complete, and most of the zinc is consumed, 40 mL of cold water is added dropwise to give a massive pale yellow finely divided precipitate. This mixture is cooled

overnight at -20 °C and then filtered to give a pale yellow/white crude solid that is dried *in vacuo*. This solid is suspended in 50 mL of hot water and heated to ~70 °C, before the unreacted zinc and zincate insoluble byproducts are filtered to give a deep yellow solution from which 0.115 g of nitrosoguanidine crystallizes on standing at 0 °C overnight. After an additional 2 days at 0 °C, more crystals are isolated by filtration to give a second crop of 0.19 g. Additional crops can be cultivated from the mother liquor with diminishing returns and purity. The total yield was 0.64 g (68% long needles). Nitrosoguanidine is readily perdeuterated, which is completely H/D exchanged, by recrystallization from D<sub>2</sub>O. DSC: *T*<sub>onset</sub> = 137 °C, *T*<sub>max</sub>(irrev) = 141.9 °C, Δ*H* = 386.1 J/g. Alternative preparations and purifications give slightly higher decomposition temperatures. For example, Thiele reports a value of ~165 °C but notes that the decomposition temperature is dependent on heating rate. In our hands, Thiele's "method I"<sup>21</sup> gives the following values: *T*<sub>onset</sub> = 153 °C, *T*<sub>max</sub>(irrev) = 156.0 °C, and Δ*H* = 333.1 J/g. Both sets of DSC data come from the same instrument running the same analysis program, that is with a heating rate of 2 °C/min. IR (KBr, cm<sup>-1</sup>): 3380.6(s), 3357.3(sh), 3130.9(s), 3099.4 (sh), 2756.7(w), 1688.7(s), 1648.8(s), 1508.2(w), 1340.6(s), 1267.0(s), 1092.4(m), 787.3(w), 690.7(m), 669.4(s), 583.7(m), 504.0(m). IR (KBr, cm<sup>-1</sup>) perdeuterated nitrosoguanidine, (D<sub>2</sub>N)<sub>2</sub>C=NNO: 2509(s), 2304(s) 1639(s), 1628(s), 1495(m) 1269(s). UV-vis H<sub>2</sub>O at pH 5.0: λ<sub>max</sub> = 259 nm (log ε = 4.86 M<sup>-1</sup> cm<sup>-1</sup>). <sup>13</sup>C NMR (*d*<sub>6</sub>-DMSO): δ 161.3. <sup>1</sup>H NMR (*d*<sub>6</sub>-DMSO): three broad singlets at δ 7.82, 7.53, and 7.11.

***N*-Methylnitrosoguanidine.** In a variation of the literature method,<sup>38,39</sup> *N*-methylnitrosoguanidine (3.45 g, 29 mmol), zinc (2.8 g, 43 mmol), and ammonium chloride (1.6 g, 30 mmol) are suspended in 10 mL of a 1:1 water/ethanol mixture. Immediately beforehand, the zinc in this reaction mixture is activated by being suspended and shaken in 0.1 M hydrochloric acid for 1 min. Following a simple decantation of the solution from the zinc, two 10 mL washes with water are employed to remove any adhering solution before adding the zinc to the reaction mixture. This mixture is stirred for 5.5 h at room temperature during which time an initial deep yellow solution forms followed by a copious white precipitate. The suspension is filtered to give a deep yellow solution that is then cooled to -22 °C. Within 30 h, deep yellow crystals of the product form that are then isolated by filtration followed by successive washes with 10 mL of cold water and 10 mL of ether. The yield of yellow needles is 0.72 g (25% yield of *N*-methylnitrosoguanidine). ESI: +ve 125.0434 for C<sub>2</sub>H<sub>6</sub>N<sub>4</sub>O<sub>2</sub>Na. DSC: *T*<sub>onset</sub> = 100.8 °C, *T*<sub>max</sub>(irrev) = 105.6 °C, and Δ*H* = 624.8 J/g (lit.<sup>38</sup> 93 °C). IR (KBr, cm<sup>-1</sup>): 3402(s), 3177(s), 2988(s), 2924(s), 2885(s), 1664.7(s), 1639.4(s), 1459.2(w), 1418.7(m), 1328.3(s), 1268.8(s), 1168.3(w), 1120.2(m), 821.4(w) 716.4(w), 585.4(m), 459.8(m). UV-vis H<sub>2</sub>O: λ<sub>max</sub> = 265 nm (log ε = 4.17 M<sup>-1</sup> cm<sup>-1</sup>), 389 nm (log ε = 1.39 M<sup>-1</sup> cm<sup>-1</sup>). <sup>13</sup>C NMR (*d*<sub>1</sub>-CDCl<sub>3</sub>): δ 164.14, 27.63. <sup>1</sup>H NMR (500 MHz, *d*<sub>6</sub>-DMSO at room temperature): three methyl doublets at δ 3.33 (<sup>3</sup>J<sub>HH</sub> = 1.2 Hz), 2.84 (<sup>3</sup>J<sub>HH</sub> = 3.7 Hz), and 2.50 (<sup>3</sup>J<sub>HH</sub> = 1.5 Hz) with a 1:1.09:1.73 ratio along with six broad singlets at δ 8.58, 8.24, 8.07, 7.47, 7.31, and 7.08 that have intensity ratios of 1:5.2, 1:5.6, 1:5.7, 1:3.3, and 1:1.0. Crystals, as a single water solvate, suitable for diffraction are grown from water.

**RuH(CO)(η<sup>2</sup>-N(O)NC(NH<sub>2</sub>)(NH))(PPh<sub>3</sub>)<sub>2</sub> (**2a**).** RuHCl(CO)(PPh<sub>3</sub>)<sub>3</sub> (0.107 g, 0.00011 mol) and nitrosoguanidine (0.035 g, 0.0004 mol, 4 equiv) are heated to reflux in 20 mL of ethanol for 20 min. Upon cooling, a fine yellow solid separates and is filtered and washed successively with 5 mL each of ethanol, water, ethanol, and hexanes. Recrystallization of this solid with dichloromethane ethanol gives 53 mg (85% yield) of pale yellow crystals of **2a**. IR (KBr, cm<sup>-1</sup>): ν(CO) 1937(s), ν(NH) 3381(m), 3344(m), 3313(m), 3166(m), 2959(w), and ν(CH) at 3056(m) with additional bands at 1660(m), 1637(m), 1591(m), 1572(m), 1332(m), 1258(w), 1217(m), 1188(m), and 874(w). <sup>1</sup>H NMR (*d*<sub>6</sub>-DMSO): δ RuH -11.97 (t, <sup>2</sup>J<sub>HP</sub> = 22.9 Hz, 1H), NH 4.35 (s, br, 1), NH 4.71 (s, br, 1), NH 5.88 (s, br, 1). <sup>31</sup>P NMR (*d*<sub>6</sub>-DMSO): δ 42.62 (s, PPh<sub>3</sub>). <sup>13</sup>C NMR (*d*<sub>6</sub>-DMSO): δ RuCO 199.4 (t, <sup>2</sup>J<sub>CP</sub> = 6.1 Hz), C(N<sub>4</sub>H<sub>3</sub>O<sub>2</sub>) 168.88(s), PCC<sub>5</sub>H<sub>5</sub> 134.64 (t, <sup>1</sup>J<sub>CP</sub> = 21.0 Hz), PCC<sub>5</sub>H<sub>5</sub> 133.93 (t, <sup>2</sup>J<sub>CP</sub> = 5.9 Hz), PCC<sub>5</sub>H<sub>5</sub> 130.52(s), PCC<sub>5</sub>H<sub>5</sub> 128.53 (t, <sup>3</sup>J<sub>CP</sub> = 4.6 Hz). DSC: *T*<sub>onset</sub> = 231 °C, *T*<sub>max</sub>(irrev) = 235.3 °C, Δ*H* = 69.2 J/g. Anal. Calcd for RuC<sub>38</sub>H<sub>34</sub>O<sub>2</sub>N<sub>4</sub>P<sub>2</sub>: C, 61.53; H, 4.62; N,

7.55. Found: C, 61.26; H, 3.91; N, 7.39. Crystals suitable for X-ray diffraction are grown from dichloromethane and ethanol.

**RuH(CO)( $\eta^2$ -N(O)NC(NH<sub>2</sub>)(NCH<sub>3</sub>))(PPh<sub>3</sub>)<sub>2</sub> (2b).** The bis-acetonitrile complex [RuH(CO)(NCCH<sub>3</sub>)<sub>2</sub>(PPh<sub>3</sub>)<sub>2</sub>]ClO<sub>4</sub> (0.173 g, 0.21 mmol) is dissolved in 5 mL of dichloromethane and diluted with 15 mL of ethanol. A solution of *N*-methylnitrosoguanidine (0.032 g, 0.31 mmol) in 10 mL of ethanol is added along with one drop of DBU. After 45 min, the dichloromethane is removed under reduced pressure and the resulting crystalline slurry concentrated to 10 mL. This mixture is filtered and washed with 2 × 10 mL of ethanol and 10 mL of hexanes to give 0.158 g of pale yellow crystals of **2b**. Yield: 98%. IR (KBr, cm<sup>-1</sup>):  $\nu$ (CO) 1925.8(s),  $\nu$ (NH) 3487(m), 3319(m), 3236(w), with the  $\nu$ (CH) at 3052(m) and with additional bands at 1635(m), 1588(m), 1316(br), and 1189(m). DSC:  $T_{\text{max}}$ (irrev) = 242.5 °C,  $\Delta H$  = 34.6 J/g. Major isomer. <sup>1</sup>H NMR (*d*<sub>2</sub>-CD<sub>2</sub>Cl<sub>2</sub>):  $\delta$  RuH -11.80 (t, <sup>3</sup>J<sub>HP</sub> = 20.9 Hz, 1H), CNCH<sub>3</sub> 1.35(s), 4.96 (brs, 1H), CNH<sub>2</sub> 4.26 (brs, 1H). <sup>31</sup>P NMR (*d*<sub>2</sub>-CD<sub>2</sub>Cl<sub>2</sub>):  $\delta$  44.92 (s, PPh<sub>3</sub>). <sup>13</sup>C NMR (*d*<sub>2</sub>-CD<sub>2</sub>Cl<sub>2</sub>):  $\delta$  RuCO 189.4 (t, <sup>2</sup>J<sub>CP</sub> = 13.1 Hz), C(CH<sub>3</sub>N<sub>4</sub>H<sub>2</sub>O<sub>2</sub>) 163.3(s), PCC<sub>5</sub>H<sub>5</sub> 134.2 (t, <sup>2</sup>J<sub>CP</sub> = 6.3 Hz), PCC<sub>5</sub>H<sub>5</sub> 129.7 (d, <sup>1</sup>J<sub>CP</sub> = 17.2 Hz), PCC<sub>5</sub>H<sub>5</sub> 129.8(s), PCC<sub>5</sub>H<sub>5</sub> 128.0 (t, <sup>2</sup>J<sub>CP</sub> = 5.2 Hz), C(CH<sub>3</sub>N<sub>4</sub>H<sub>3</sub>O<sub>2</sub>) 36.5(s). Minor isomer. <sup>1</sup>H NMR (*d*<sub>2</sub>-CD<sub>2</sub>Cl<sub>2</sub>):  $\delta$  RuH -11.95 (t, <sup>3</sup>J<sub>HP</sub> = 22.1 Hz, 1H), CNHCH<sub>3</sub> 2.10 (d, <sup>2</sup>J<sub>HH</sub> = 5.05 Hz, 3H), 4.96 (brs, 1H), CNH<sub>2</sub> 4.26 (brs, 1H). <sup>31</sup>P NMR (*d*<sub>2</sub>-CD<sub>2</sub>Cl<sub>2</sub>):  $\delta$  44.38 (s, PPh<sub>3</sub>). <sup>13</sup>C NMR (*d*<sub>2</sub>-CD<sub>2</sub>Cl<sub>2</sub>):  $\delta$  RuCO 196.5 (t, <sup>2</sup>J<sub>CP</sub> = 18.0 Hz), C(CH<sub>3</sub>N<sub>4</sub>H<sub>2</sub>O<sub>2</sub>) 167.3(s), PCC<sub>5</sub>H<sub>5</sub> 134.0 (t, <sup>2</sup>J<sub>CP</sub> = 6.1 Hz), PCC<sub>5</sub>H<sub>5</sub> 131.9 (d, <sup>1</sup>J<sub>CP</sub> = 10.1 Hz), PCC<sub>5</sub>H<sub>5</sub> 133.8 (s), PCC<sub>5</sub>H<sub>5</sub> 127.9 (t, <sup>2</sup>J<sub>CP</sub> = 5.5 Hz), C(CH<sub>3</sub>N<sub>4</sub>H<sub>3</sub>O<sub>2</sub>) 26.5 (s). Anal. Calcd for RuClC<sub>38</sub>H<sub>33</sub>O<sub>2</sub>N<sub>4</sub>P<sub>2</sub>: C, 58.80; H, 4.29; N, 7.23. Found: C, 58.46; H, 4.67; N, 7.42. Crystals suitable for X-ray diffraction are grown from dichloromethane and ethanol.

**RuCl(CO)( $\eta^2$ -N(O)NC(NH<sub>2</sub>)(NH))(PPh<sub>3</sub>)<sub>2</sub> (3a).** Hydride complex **2a**, RuH(CO)( $\eta^2$ -N(O)NC(NH<sub>2</sub>)(NH))(PPh<sub>3</sub>)<sub>2</sub> (0.065 g, 0.088 mmol), is suspended in a 10:1 mixture of chloroform and carbon tetrachloride and brought to reflux for 5 h. Upon cooling, a fine yellow solid separates. The volatiles are removed, and the crystalline residue is suspended in 20 mL of ethanol, filtered, and washed successively with 5 mL each of ethanol, water, ethanol, and finally hexanes. Recrystallization of this solid with dichloromethane ethanol gives 58 mg (85% yield) of bright lime-yellow crystals of **3a**. IR (KBr, cm<sup>-1</sup>):  $\nu$ (CO) 1958(s),  $\nu$ (NH) 3470(m), 3375(m), 3236(w), 3133(m), 2968(w), and  $\nu$ (CH) 3056(m) and with additional bands at 1634(m), 1573(m), 1403(m), 1372(br), 1187(m), and 803(w). DSC:  $T_{\text{onset}}$  = 253 °C,  $T_{\text{max}}$ (irrev) = 255.9 °C,  $\Delta H$  = 68.8 J/g. <sup>1</sup>H NMR (*d*<sub>1</sub>-CDCl<sub>3</sub>):  $\delta$  RuNH 4.96 (brs, 1H), CNH<sub>2</sub> 4.26 (brs, 1H). <sup>31</sup>P NMR (*d*<sub>1</sub>-CDCl<sub>3</sub>):  $\delta$  29.28 (s, PPh<sub>3</sub>). <sup>13</sup>C NMR (*d*<sub>6</sub>-DMSO):  $\delta$  RuCO 188.9 (t, <sup>2</sup>J<sub>CP</sub> = 12.4 Hz), C(N<sub>4</sub>H<sub>3</sub>O<sub>2</sub>) 167.8 (s), PCC<sub>5</sub>H<sub>5</sub> 131.5 (t, <sup>1</sup>J<sub>CP</sub> = 21.4 Hz), PCC<sub>5</sub>H<sub>5</sub> 128.3 (d, <sup>2</sup>J<sub>CP</sub> = 4.7 Hz), PCC<sub>5</sub>H<sub>5</sub> 134.4 (s), PCC<sub>5</sub>H<sub>5</sub> 130.5 (s). Anal. Calcd for RuClC<sub>38</sub>H<sub>33</sub>O<sub>2</sub>N<sub>4</sub>P<sub>2</sub>: C, 58.80; H, 4.29; N, 7.23. Found: C, 58.46; H, 4.67; N, 7.42. Crystals suitable for X-ray diffraction are grown from dichloromethane and ethanol.

**RuCl(CO)( $\eta^2$ -N(O)NC(NMeH)(NH))(PPh<sub>3</sub>)<sub>2</sub> (3b).** Hydride complex **3a**, RuH(CO)( $\eta^2$ -N(O)NC(NH<sub>2</sub>)(NMe))(PPh<sub>3</sub>)<sub>2</sub> (0.052 g, 6.5 mmol), is dissolved in 20 mL of dichloromethane, treated with *N*-chlorosuccinimide (19 mg, 14 mmol, 2.8 equiv), and stirred at room temperature for 68 h. The resulting orange/yellow solution is diluted with 20 mL of ethanol, turning pale yellow, and recrystallized by concentration to 5 mL. The resulting crystal mass is filtered and washed with 3 × 10 mL of ethanol to give 41 mg of the crude solid. Recrystallization of this solid with dichloromethane ethanol gives 38 mg (5.1 mmol, 79% yield) of pale bright lime-yellow crystals of **3b**. IR (KBr, cm<sup>-1</sup>):  $\nu$ (CO) 1951(s),  $\nu$ (NH) 3406(m), 3141(w), 2964(w) and  $\nu$ (CH) 3051(m) and with additional bands at 1656(m), 1627(m), 1607(m), 1402(w), 1363(br), 1230(m), and 1187(m). DSC:  $T_{\text{onset}}$  = 276 °C,  $T_{\text{max}}$ (irrev) = 278 °C,  $\Delta H$  = 1.4 J/g. <sup>1</sup>H NMR (*d*<sub>1</sub>-CDCl<sub>3</sub>):  $\delta$  RuNH 4.96 (brs, 1H), CNH<sub>2</sub> 4.26 (brs, 1H). <sup>31</sup>P NMR (*d*<sub>1</sub>-CDCl<sub>3</sub>):  $\delta$  29.28 (s, PPh<sub>3</sub>). <sup>13</sup>C NMR (*d*<sub>6</sub>-DMSO):  $\delta$  RuCO 207.0 (s), C(MeCN<sub>4</sub>H<sub>2</sub>O) 165.3 (s), PCC<sub>5</sub>H<sub>5</sub> 131.9 (t, <sup>1</sup>J<sub>CP</sub> = 21.3 Hz), PCC<sub>5</sub>H<sub>5</sub> 128.6 (t, <sup>2</sup>J<sub>CP</sub> = 4.6 Hz), PCC<sub>5</sub>H<sub>5</sub> 134.4 (t, <sup>2</sup>J<sub>CP</sub> = 5.3 Hz), PCC<sub>5</sub>H<sub>5</sub> 130.6 (s), C(MeCN<sub>4</sub>H<sub>2</sub>O) 30.0 (s). Anal. Calcd for RuClC<sub>39</sub>H<sub>35</sub>O<sub>2</sub>N<sub>4</sub>P<sub>2</sub>: C, 59.28; H, 4.46; N, 7.09. Found: C, 59.06; H,

4.61; N, 7.23. Crystals suitable for X-ray diffraction are grown from dichloromethane and ethanol.

**Ru(Ph)(CO)( $\eta^2$ -N(O)NC(NH<sub>2</sub>)(NH))(PPh<sub>3</sub>)<sub>2</sub> (4a).** RuCl(Ph)(CO)-(PPh<sub>3</sub>)<sub>2</sub> (116 mg, 0.15 mmol) is dissolved in 20 mL of dichloromethane and treated with one drop of 1,8-diazabicyclo[5.4.0]undec-7-ene (DBU, neat). A solution of nitrosoguanidine (17 mg, 0.2 mmol) is dissolved with heating in 2 mL of water and then diluted with 20 mL of ethanol before being added rapidly in one aliquot to the ruthenium complex. Within 30 min the solution turns from light red to pale yellow, with the formation of an off-white precipitate. This suspension is concentrated and diluted with fresh ethanol to give a final suspension under a volume of 10 mL of ethanol and water. Filtration followed by successive washes with water, ethanol, and hexane gives an off-white solid that can be further purified by recrystallization from dichloromethane and ethanol to give 87 mg (73% yield) of pale yellow crystals of **4a**. IR (KBr, cm<sup>-1</sup>):  $\nu$ (CO) 1940(s),  $\nu$ (NH) 3426(m), 3329(m), 3236(w), 3133(m), 2968(w), and  $\nu$ (CH) 3054(m) and with additional bands at 1648(m), 1586(w), 1566(m), 1385(m), 1293(br), and 1185(m). DSC:  $T_{\text{onset}}$  = 228 °C,  $T_{\text{max}}$ (irrev) = 229.8 °C,  $\Delta H$  = 18.5 J/g. <sup>1</sup>H NMR (*d*<sub>6</sub>-DMSO):  $\delta$  P(C<sub>6</sub>H<sub>5</sub>)<sub>3</sub> 7.34 (t, 6H, <sup>3</sup>J<sub>HH</sub> = 7.1 Hz), 7.25 (t, 12H, <sup>3</sup>J<sub>HH</sub> = 7.5 Hz), 7.17 (m, 12H), RuNH 6.04 (brs, 1H), CNH<sub>2</sub> 7.44 (brs, 2H), RuCC-H 6.79 (d, 2H, <sup>3</sup>J<sub>HH</sub> = 7.4 Hz), RuCCCCH 6.45 (t, 1H, <sup>3</sup>J<sub>HH</sub> = 7.1 Hz), RuCCCH 6.27 (t, 2H, <sup>3</sup>J<sub>HH</sub> = 7.3 Hz). <sup>31</sup>P NMR (*d*<sub>1</sub>-CDCl<sub>3</sub>):  $\delta$  29.28 (s, PPh<sub>3</sub>). <sup>31</sup>P NMR (*d*<sub>6</sub>-DMSO):  $\delta$  31.06 (s, PPh<sub>3</sub>). <sup>13</sup>C NMR (*d*<sub>6</sub>-DMSO):  $\delta$  RuCO 207.0 (s), C(N<sub>4</sub>H<sub>3</sub>O<sub>2</sub>) 168.5 (s), PCC<sub>5</sub>H<sub>5</sub> 132.7 (t, <sup>1</sup>J<sub>CP</sub> = 20.7 Hz), PCC<sub>5</sub>H<sub>5</sub> 128.1 (t, <sup>2</sup>J<sub>CP</sub> = 4.4 Hz), PCC<sub>5</sub>H<sub>5</sub> 134.1 (t, <sup>2</sup>J<sub>CP</sub> = 5.2 Hz), 129.9 (s), PCC<sub>5</sub>H<sub>5</sub> 130.5 (s), RuCC<sub>3</sub>H<sub>5</sub> 145.4, 134.1, 125.4, 121.0. Anal. Calcd for RuClC<sub>38</sub>H<sub>33</sub>O<sub>2</sub>N<sub>4</sub>P<sub>2</sub>: C, 58.80; H, 4.29; N, 7.23. Found: C, 58.46; H, 4.67; N, 7.42. Crystals suitable for X-ray diffraction are grown from dichloromethane and ethanol.

**Ru(Ph)(CO)( $\eta^2$ -N(O)NC(NH<sub>2</sub>)(NCH<sub>3</sub>))(PPh<sub>3</sub>)<sub>2</sub> (4b).** RuCl(Ph)(CO)-(PPh<sub>3</sub>)<sub>2</sub> (140 mg, 0.15 mmol) is dissolved in 20 mL of dichloromethane, treated with a solution of *N*-methylnitrosoguanidine (26 mg, 1.2 equiv, 0.25 mmol), dissolved in 30  $\mu$ L of water, with heating, and diluted with 20 mL of ethanol and one drop of 1,8-diazabicyclo[5.4.0]undec-7-ene (DBU, neat). Within 30 min, the solution turns from light red to dirty brown-yellow. This solution is concentrated and diluted with fresh ethanol to give a final crystallizing suspension with a volume of <10 mL. After cooling at -20 °C for 3 days, the resulting yellow crystal mass is filtered and washed successively with water, ethanol, and hexane to give an off-white solid that can be further purified by recrystallization from dichloromethane and ethanol to give 78 mg (45% yield) of pale yellow crystals of **4b**. IR (KBr, cm<sup>-1</sup>):  $\nu$ (CO) 1937(s),  $\nu$ (NH) 3438(m), 3386(m), 3206(w), 2966(w), and  $\nu$ (CH) 3054(m) with additional bands at 1629(m), 1602(m), 1561(m), 1349(m), 1331(m), 1255(m), 1239(br), and 1188(m). DSC:  $T_{\text{onset}}$  = 156 °C,  $T_{\text{max}}$ (irrev) = 158.9 °C,  $\Delta H$  = -18.4 J/g. <sup>1</sup>H NMR (*d*<sub>6</sub>-DMSO):  $\delta$  P(C<sub>6</sub>H<sub>5</sub>)<sub>3</sub> 7.34 (m, 6), 7.23 (m, 12), 7.13 (m, 12), Ru-CCH 7.03 (d, 2, <sup>2</sup>J<sub>HH</sub> = 7.3 Hz), Ru-CCC-H 6.67 (t, 2H, <sup>1</sup>J<sub>HH</sub> = 7.0 Hz), Ru-CCCCH 6.80 (t, 1H, <sup>1</sup>J<sub>HH</sub> = 6.9 Hz), RuNH 4.96 (brs, 1H), CNH<sub>2</sub> 4.26 (brs, 1H). <sup>31</sup>P NMR (*d*<sub>6</sub>-DMSO):  $\delta$  29.68 (s, PPh<sub>3</sub>). <sup>13</sup>C NMR (*d*<sub>6</sub>-DMSO):  $\delta$  RuCO 204.3 (t, <sup>2</sup>J<sub>CP</sub> = 16.3 Hz), C(MeCN<sub>4</sub>H<sub>2</sub>O) 167.9 (s), Ru(CC<sub>5</sub>H<sub>5</sub>) 158.7 (s), 144.0 (s), 126.2 (s), 121.7 (s), PCC<sub>5</sub>H<sub>5</sub> 132.7 (t, <sup>1</sup>J<sub>CP</sub> = 20.3 Hz), PCC<sub>5</sub>H<sub>5</sub> 128.1 (t, <sup>2</sup>J<sub>CP</sub> = 4.2 Hz), PCC<sub>5</sub>H<sub>5</sub> 134.4 (t, <sup>2</sup>J<sub>CP</sub> = 4.9 Hz), PCC<sub>5</sub>H<sub>5</sub> 130.1 (s), C(MeCN<sub>4</sub>H<sub>2</sub>O) 34.28 (s). Anal. Calcd for RuC<sub>45</sub>H<sub>33</sub>O<sub>2</sub>N<sub>4</sub>P<sub>2</sub>: C, 64.74; H, 5.19; N, 6.71. Found: C, 64.82; H, 5.33; N, 6.82. Crystals suitable for X-ray diffraction are grown from dichloromethane and ethanol.

**Theoretical Methods.** Density functional theory implemented on Gaussian16 with B3LYP functionals is used with cc-pvdz, cc-pvtz, and aug-cc-pvtz basis sets. For calculations of the ruthenium complexes, effective core potentials based on a fully relativistic multielectron fit of 28 core electrons are used.<sup>40</sup>

**X-ray Crystallography.** Crystals are mounted on glass fibers with epoxy resin or Mitogen mounts using Paratone-N oil from Hampton Research, and single-crystal X-ray diffraction experiments are carried out with a BRUKER APEX-II CCD D8 diffractometer by using graphite-monochromated Mo K $\alpha$  radiation ( $\lambda$  = 0.71073 Å) and

KRYOFLEX for low-temperature experiments. APEXII<sup>41</sup> is used to integrate the intensity reflections, and scaling and SADABS<sup>42</sup> for absorption correction. A combination of intrinsic phasing and direct methods is used to determine the structure that is subsequently anisotropically refined after all non-hydrogen atoms are located by difference Fourier maps, and final solution refinements are determined by a full-matrix least-squares method on  $F^2$  of all data, by using SHELXTL.<sup>41</sup> The hydrogen atoms are placed in calculated positions.

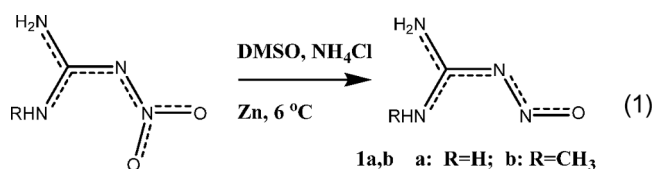
Nitrosoguanidine and its complexes are often strongly hydrogen bonded and/or solvated, particularly for the complexed noncoordinated NHR group. In some cases, the crystallographic solvates associated with this site are well-defined, but often modeling the electron density of the solvate is critical for determining the best overall fit for the data. For example, in the case of parent hydride complex **2a**, and the related phenyl derivative **2c**, a single ethanol hydrogen bonds to the NH<sub>2</sub> group of the nitrosoguanidine ligand. In **2a**, the solvate is disordered between two sites, while in **2c**, it is well-defined in one location. A consequence of this disorder is that in **2c** a complete ethanol model is possible to refine, with hydrogen atom positions, but in **2a** the hydrogen atoms have not been included. In the *N*-methylnitrosoguanidine structure, a water solvate is apparent from the electron density difference maps and the data are of such high quality that reasonable positions for all of the hydrogen atoms are apparent in the latter stage of the refinement and are included and refined from the experimental positions in the final electron density model. Crystallographic data have been supplied to the CCDC and are available with the deposition codes as delineated in Table S3.

## RESULTS AND DISCUSSION

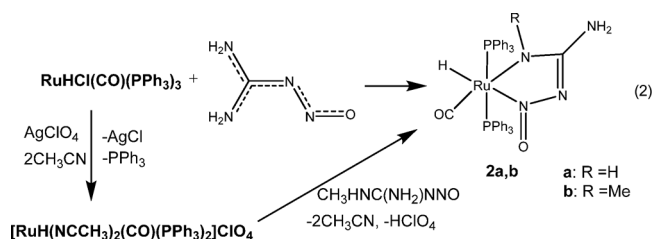
**Synthesis of Nitrosoguanidine, Methylnitrosoguanidine, and Their Complexes.** Although nitrosoguanidine **1a** is readily prepared by aqueous zinc reduction at increased temperatures,<sup>21,43,44</sup> the yield is markedly dependent upon conditions. The original figure of 38%<sup>21</sup> is seldom matched by more recent reports that typically return values of <8%. This poor yield is offset by the ease of isolation of nitrosoguanidine by recrystallization from cold water. The origin of this difficulty stems ultimately from the over-reduction of nitroguanidine to aminoguanidine and the general thermal instability of this class of guanidines. Thiele encountered this problem in his seminal clarification of the constitution of nitroguanidine, which had beforehand been formulated as the nitroso derivative.<sup>33,45</sup> Although within a year he described the isolation and characterization of nitrosoguanidine, in his initial publication<sup>21</sup> he only outlined the properties of the nitrosoguanidine intermediate during reduction but did not attribute its presence to these reductions.<sup>45</sup> In addition to these competing reductions of nitro- and nitrosoguanidine is the complication of the low solubility of both the starting material and its first reduction product. Thiele describes an acid/base workup<sup>21</sup> that can be used to separate nitro- and nitrosoguanidine and exploits the latter's relative basicity with a  $pK_b$  of 11.90.<sup>46</sup> The reduction of nitroguanidine with Pt/H<sub>2</sub> has been reported, but again the over-reduction to aminoguanidine is a significant side product.<sup>47,48</sup> In addition to these difficulties, the conditions for zinc reduction in water used for nitrosoguanidine cannot be generalized to other alkylnitrosoguanidines.

A straightforward resolution to these difficulties is the use of non-aqueous conditions, in particular DMSO or ethanol as the solvent for the reduction. Under these conditions, both nitroso- and nitroguanidines are readily soluble in DMSO and treatment with a slight excess of zinc powder results in the rapid formation of a deep yellow solution of the nitrosoguanidine product. Isolation of the nitrosoguanidine product is readily accomplished by precipitation with cold water, cooling, and filtration of

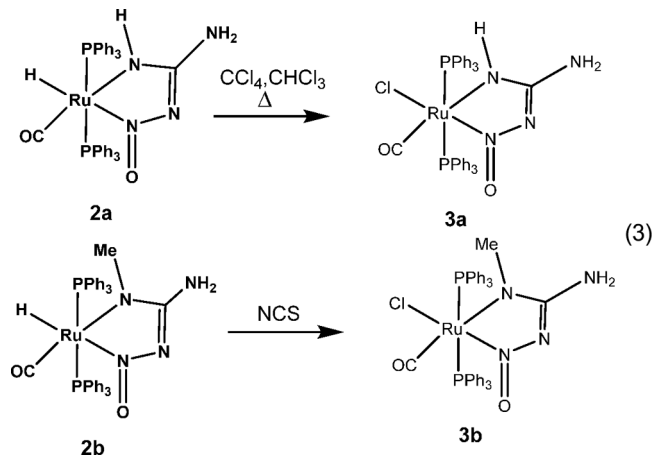
the insoluble product (eq 1). In the case of *N*-methylnitrosoguanidine, a better yield of the isolated product is obtained when

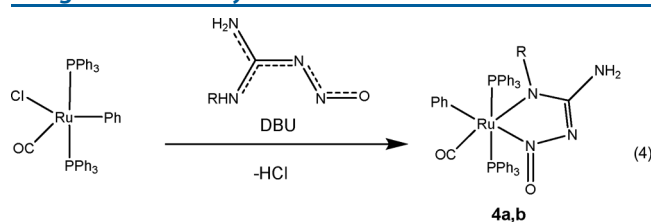


ethanol is used as the reduction medium. Nitrosation and nitration of guanidine decrease the basicity of the conjugate base of guanidinium salt so that these products are typically isolated as neutral solids. However, the remaining guanidine protons have sufficient acidity, so that coordination of nitrosoguanidine allows for the formation of an anionic nitrosoguanidinate anion. In the reaction of RNHC(NH<sub>2</sub>)NNO with RuHCl(CO)(PPh<sub>3</sub>)<sub>3</sub> (eq 2), coordination follows loss of HCl, along with a



labile PPh<sub>3</sub>, to give **2a** as a single isomer with *trans* triphenylphosphines. Although **2a** has only modest solubility in most organic solvents, it is readily purified by recrystallization from dichloromethane and diffraction grade crystals can be obtained from this solvent. Chlorination of **2a** and **2b** to give **3a** and **3b**, respectively, occurs in chloroform at increased temperatures (eq 3). While this is a convenient method for the preparation of RuCl(NGD)(CO)(PPh<sub>3</sub>)<sub>2</sub> (**3a**), the reaction fails for the preparation of pure methyl analogue **3b**, which is instead best prepared by treating **2b** with *N*-chlorosuccinimide (NCS). Treating RuCl(Ph)(CO)(PPh<sub>3</sub>)<sub>2</sub> with RNHC(NH<sub>2</sub>)NNO gives predominately phenyl derivatives **4a** and **4b** (eq 4), but there is substantial competing elimination of benzene to return the corresponding chloride complexes **3a** and **3b**, respectively. In this case, there is competition for the elimination of HCl or H-Ph from the complex, and this is diminished with the addition of the strong base DBU. Here the **4a/4b** and **3a/3b** mixtures are readily separated by recrystallization given the poorer solubilities of chlorides **3a** and **3b**.





**Structure, Conformational Dynamics, and Spectroscopy of the Nitrosoguanidines.** The planar delocalized bonding in the guanidyl moiety gives rise to restricted C–N rotation, acidic N–H groups, and an associated weak or diminished basicity of the amine. Nitration and nitrosation of guanidine decrease this basicity further to the point where the two adducts are isolated as uncharged molecules. The single-crystal structure of methylnitrosoguanidine hydrate has been measured with X-ray diffraction (Figure 1 and Tables S1 and S2)

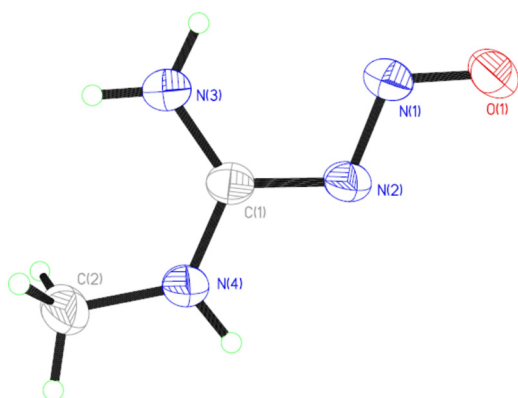


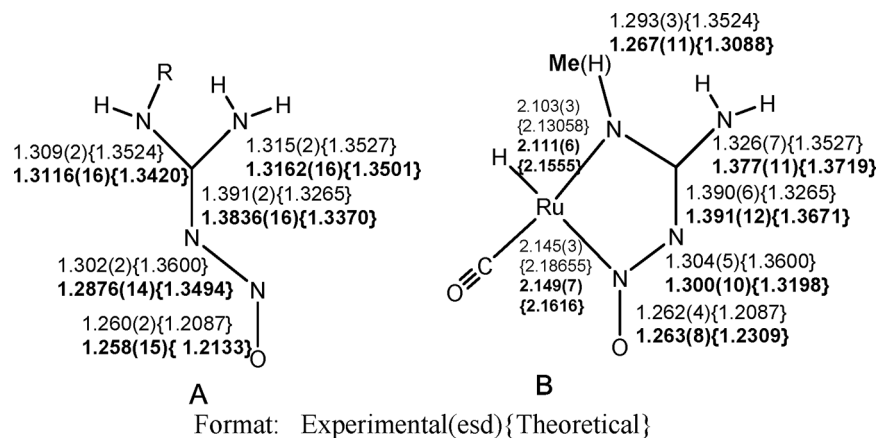
**Figure 1.** Single-crystal X-ray diffraction structure of methylnitrosoguanidine (**1b**) as the EEE conformation. Water solvate not shown. Key metric parameters are included in Figure 2, and 40% thermal ellipsoids are shown in this and other ORTEP plots.

and corresponds to a single planar conformation with an EEE arrangement around N1, N2, and C1. As shown in Figure S1, there is an extensive intermolecular hydrogen bonding network between the N–H and OH<sub>2</sub> groups and O1, N1, and N2. As

shown in Figure 2A, the hydrogen bonding present in the solid state leads to marked changes in the bonding as compared to that of the gas phase structure calculated at the B3LYP/aug-cc-pvtz level of theory. In particular, the substantial decrease in the N–N bond length and the corresponding increase in the C–NN bond length reflect these hydrogen bonds.

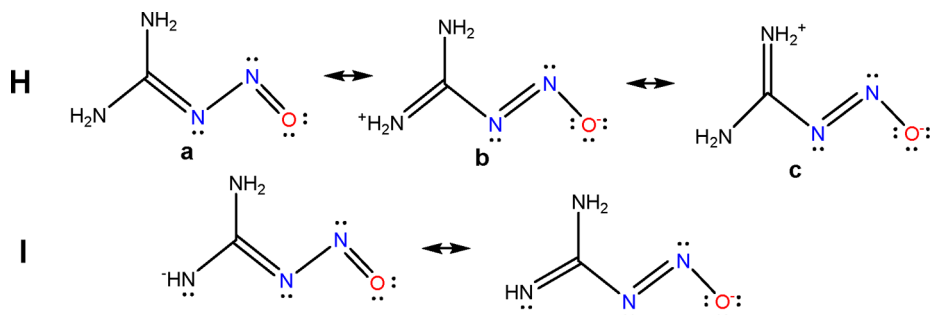
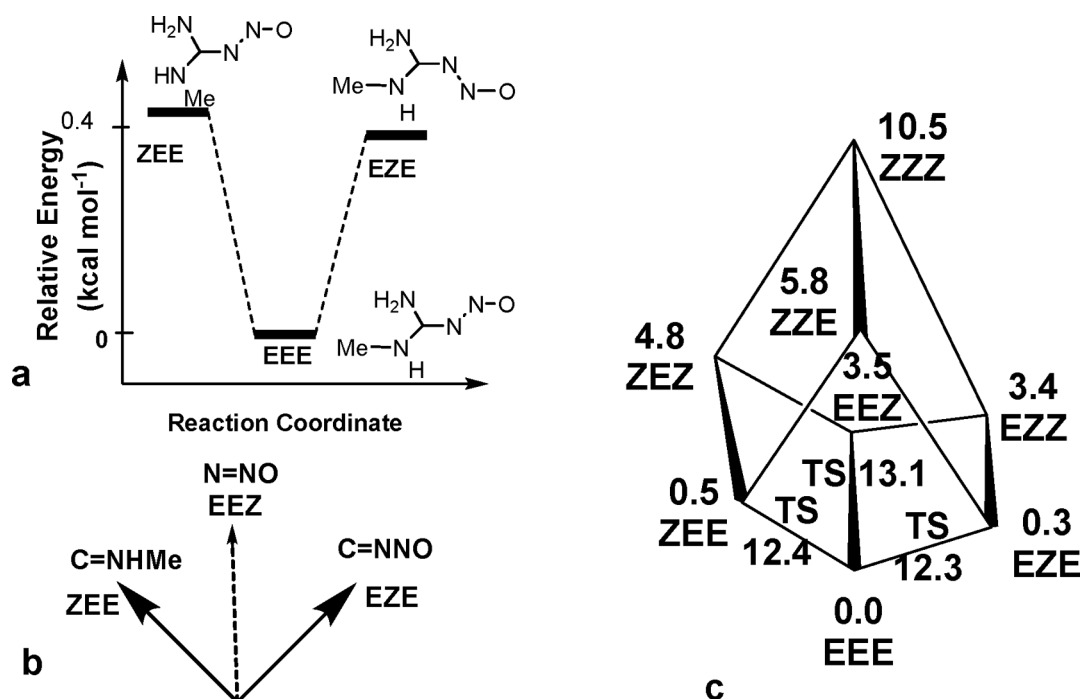
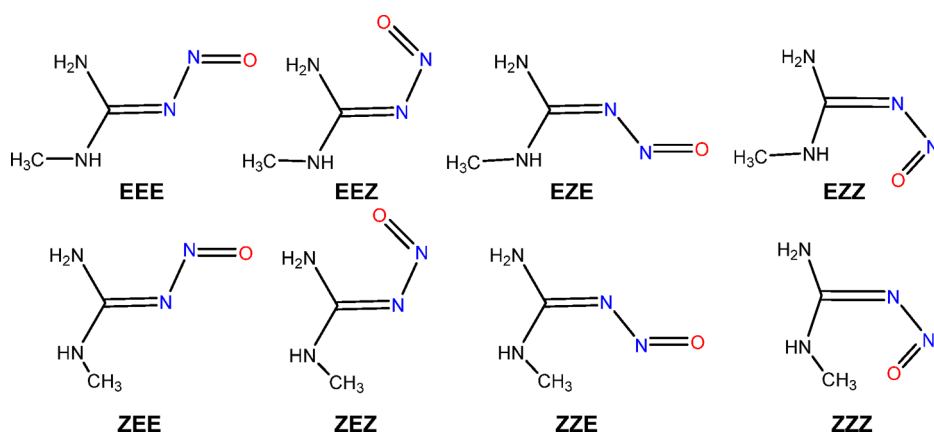
Similar patterns in the metric parameters are seen for the parent nitrosoguanidine structure.<sup>14</sup> This hydrogen bonding network leads to some marked changes in bonding, which in terms of Lewis diagrams corresponds to an increased contribution of resonance form **Hb** (Scheme 1). The planarity and delocalization result in configurationally significant rotation barriers around the central N–C and N–N bonds. The expectation from Lewis diagrams (Scheme 1) is that the anion **I**, as a ligand, should be a good  $\pi$ -acceptor at the nitroso position and possibly a  $\pi$ -donor at the NR position. Thus, they may be amphoteric chelates in their ability to  $\pi$ -accept and donate within the same ligand. Alternatively, they can be viewed as metallocenolates.

For **1a** and **1b**, the solid state conformations correspond to an E geometry with respect to the C–N–N–O torsion angles. For nitrosoguanidine, these stereochemical dynamics correspond to E/Z, rotation around the C–N–N–O torsion angle (Scheme 2). Monomethylation creates two new E/Z stereocenters, each with E/Z conformers around the N bearing the methyl and the central carbon (Figure 1). For **1b**, the crystallographically determined structure with a hydrogen-bonded water corresponds to the EEE stereoisomer (Scheme 2). Dissolution of these crystals into solvents such as DMSO, water, chloroform, and ethanol give variable and different ratios of methyl resonances in their <sup>1</sup>H NMR spectra. These spectra are also dependent on concentration and temperature with some impurity-dependent variability. In contrast, in the <sup>13</sup>C NMR spectra for **1a**, only a single guanidinyll resonance is measured, while for **1b**, there are two predominant resonances. The same spectra for **1b** are obtained when diffraction grade crystals are dissolved and measured, and also when the CDCl<sub>3</sub> solution is quickly warmed to reflux, cooled, and measured again. Clearly, the configurational equilibrium in **1b** is attained at room temperature.



**Figure 2.** Crystal and theoretical (DFT) structures for the free ligand metric parameters for nitrosoguanidine in plain text and (A) *N*-methylnitrosoguanidine in bold text and (B) the ruthenium complexes RuH(CO)(RNGD)(PPh<sub>3</sub>)<sub>2</sub>. In panel A, the EEE structure is found in the solid state of *N*-methylnitrosoguanidine (**1b**), and this is contrasted with the E geometry found by Murman et al. The calculated distances, in braces, correspond to the B3LYP/aug-cc-pvtz level. In panel B, the view is along the Ph<sub>3</sub>P–Ru–PP<sub>3</sub> axis with the RNGD ligands adopting an EZE geometry. Here the crystallographic metric parameters are shown first with the calculated values in braces for the corresponding RuH(CO)(RNGD)(PMe<sub>3</sub>)<sub>2</sub> complexes. Calculated values from the B3LYP/cc-pvtz level for all non-metal atoms and with a pseudopotential for Ru.

Scheme 1. Lewis Structure of Nitrosoguanidine (H) and Its Conjugate (I)

Scheme 2. Conformational Isomers of *N*-Methylnitrosoguanidine

**Figure 3.** Calculated (B3LYP/aug-cc-pvtz) gas phase total electronic energies for MeNHC(NH<sub>2</sub>)NNO. Relative energies and the three lowest configurations shown in kilocalories per mole are shown in panel a. (b and c) Graphic representations<sup>49</sup> for the six stereoisomers, their relative energies, and the barriers for interconversion. The stereochemistry from Scheme 2 is shown under each graph vertex with EEE as the minimum, and the three transition barriers for EEE to EZE, EEZ, and ZEE are shown along the tie line. The original cube is shown distorted to reflect the relative energies and the three axes for isomerization shown in 1b.

The dynamic landscape of eight Z/E/E conformers (Figure 3) has been theoretically modeled in the gas phase with DFT (B3LYP/aug-cc-PVDZ). The relative energies of the different

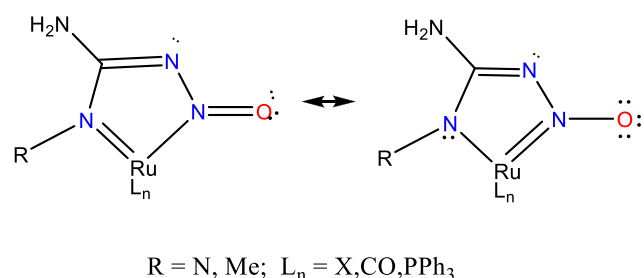
isomers along with the rotational/interconversion barriers are depicted in Figure 3. The lowest-energy gas phase conformation, EEE, corresponds to the observed solid state structure, but the

complexity of the  $^1\text{H}$  and  $^{13}\text{C}$  NMR spectra corresponds to three species with a ratio of 1:1.09:1.73 in DMSO at room temperature; however, only six signals due to the N–H protons are observed, and in the  $^{13}\text{C}$  spectra, only two methyl resonances are seen.

Time-dependent DFT (B3LYP/aug-cc-pvtz) was used to gauge the dependence of the intense  $n \rightarrow \pi^*$  UV–vis band as a function of both conformation and, separately, solvent (Table S1). It was proposed that the solvatochromism and the energy of the band might reflect the equilibrium geometries present in solution. However, the observed band at 265 nm has little solvent dependency and the predicted weak band at  $\sim 500$  nm is not observed. There is little indication of multiple conformations in solution by these bands alone.

**Coordination Chemistry of the Nitrosoguanidines and Formation and Characterization of 2,3,5-Rutheniatriazoles.** A common feature of all of these complexes is the presence of a Ru–N bond to the nitroso group and chelation/metalation to one of the other guanidinyll nitrogens to give planar five-membered rings. In addition, the nitroso group is consistently *cis* to the carbonyl and *trans* to the anionic donor. Ligand-delocalized bonding accompanies ruthenium nitrogen multiple-bond interactions, with both  $\pi$ -accepting and -donating interactions shown in Scheme 3. In this model,  $\pi$ -back-bonding

Scheme 3



to the nitroso group in one contribution is balanced by  $\pi$ -donation from the amido nitrogen to the metal. Complexes **2a** and **2b** share the coordination preference for *cis*  $\pi$ -accepting ligands with the  $\pi$ -donating amido nitrogen *trans* to the carbonyl. The solid state structural geometries for the hydride complexes are shown in Figure 4, and metric parameters are collected and contrasted in Figure 2 and Table 1.

Hydrides often exert a strong *trans* influence in the carbonyl phosphine complexes of Ru(II), and the effect of the hydride on the nitroso group *trans* to it can be seen by comparison with the closely related chloride, **3a** and **3b** (Figure 5), as the chlorides have differences in their Ru–N bond lengths of  $\lesssim 0.15$  Å. For the corresponding phenyl complexes, **4a** and **4b**, shown in Figure 6, the strong *trans* influence of the aryl groups is shown with increased Ru–N distances for both Ru–N bond lengths in both nitrosoguanidines in **4a** and **4b**. Excellent gauges of the electronic effects of the nitrosoguanidines are the carbonyl stretching frequencies (Table 1, which vary by  $\sim 30$   $\text{cm}^{-1}$  depending on the metal-bound anion ( $\text{Cl} > \text{Ph} > \text{H}$ ) and nitrosoguanidine versus methyl nitrosoguanidine. A complication in interpreting the energies of these bands is that coupling of the H–Ru–CO modes in **2a** and **2b** is likely to be strong and only a single band is observed for these hydride complexes; there is no evidence for a band corresponding to a separate  $\nu(\text{Ru–H})$  mode. Nevertheless, each proto/methyl nitrosoguanidine pair

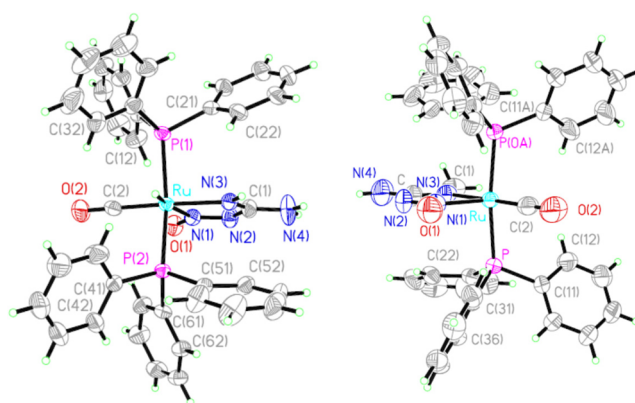


**Figure 4.** ORTEP representations for the crystal structures of **2a** (left) and **2b** (right). All of the ruthenium complex diagrams are drawn with 40% thermal ellipsoids. The hydride ligand was not located or modeled in **2b** in the final refinement and has been omitted from the diagram.

has lower  $\nu(\text{Ru–C=O})$  values corresponding to more electron density being donated to the metal by the methyl nitrosoguanidine.

Perhaps the most significant structural trends that accompany binding of nitrosoguanidine and methyl nitrosoguanidine are associated with the guanidinyll fragment. The ONNC fragments have metric parameters that are scattered around the same values as in the free ligand. For the guanidinyll fragment, however, metal binding leads to a decrease in the RuN(R)–C and RuN(R)C–NH<sub>2</sub> distances where there is a net increase in the N(3)–C bond order and a decrease in the C–N(4)H<sub>2</sub> bond order. In all cases, however, the bond lengths remain in the range of those known for C=N, albeit at the longer end of that range. Taken together, the presence of extensive delocalized bonding within the chelate rings, along with their planarity, supports the formulation of these complexes as metallotriazoles.

The reactivity of these chelates is related to the intrinsic stability of these types of heterocycles. These adducts have high thermal stability, with many decomposing after heating to only  $>250$  °C, and there is only one indication that the chelate can be ruptured; however, this is in chemistry associated with the osmium analogue of **2a** that slowly decomposes at room temperature to give the nitrosyl complex OsCl(CO)(NO)(PPh<sub>3</sub>)<sub>2</sub>. The other byproducts of this degradation remain to be determined, and this chemistry will be reported elsewhere.

## CONCLUSION

Given the robustness of the six nitrosoguanidine complexes prepared and characterized in this report, it is at first glance surprising how little precedent there is for this class of strong chelating ligand. Certainly some of this paucity is due to issues of solubility and poor synthetic access. In the case of the parent ruthenium nitrosoguanidine complexes prepared here, the mutually *trans* triphenylphosphine ligands minimize some of the strong hydrogen bonding networks that contribute to the insolubility of prior complexes. With the development of these improved preparations and new coordination chemistry of the *N*-methyl nitrosoguanidine complexes reported here, there potentially are many other mono- and perhaps dialkylated nitrosoguanidines that can be prepared using these non-aqueous synthetic methods. The complexes reported here are all  $d^6$  18-electron species with relatively inert coordination environments. Nevertheless, in two of these examples, the nitroso group is bound *trans* to excellent *trans*-influencing ligands in the cases of

Table 1. Selected Metrics (angstroms or degrees) and Vibrational Parameters for Ruthenium Nitrosoguanidine Complexes

	1a <sup>a</sup>	1b	2a	2b	3a <sup>b</sup>	3b	4a	4b <sup>b</sup>
Ru–N(1)	–		2.145(3)	2.149(7)	1.989(14)	2.007(8)	2.162(3)	2.099(1)
Ru–N(3)	–		2.103(3)	2.111(6)	2.072(1)	2.086(8)	2.098(3)	2.141(1)
N(1)–O	1.260(2)	1.258(15)	1.262(4)	1.263(8)	1.225(7)	1.243(9)	1.267(3)	1.257(1)
N(1)–N(2)	1.302(2)	1.2876(14)	1.304(5)	1.300(10)	1.331(2)	1.287(10)	1.301(4)	1.308(3)
N(2)–C	1.391(2)	1.3836(16)	1.390(6)	1.391(12)	1.371(2)	1.404(13)	1.381(4)	1.397(13)
C–N(3)	1.309(2)	1.3116(16)	1.293(3)	1.267(11)	1.276(7)	1.301(12)	1.285(4)	1.304(7)
C–N(4)	1.315(2)	1.3162(16)	1.326(7)	1.377(11)	1.336(8)	1.348(12)	1.351(4)	1.344(7)
O–N(1)–N(2)		114.14(10)	114.83(4)	115.31(7)	115.56(96)	114.61(9)	114.5(3)	114.41(3)
N(1)–N(2)–C		111.55(10)	110.19(4)	111.29(7)	112.24(60)	110.79(9)	110.6(3)	109.71(59)
N(2)–C–N(4)		123.44(10)	113.83(5)	112.89(9)	115.02(41)	111.89(11)	114.6(3)	111.71(56)
N(3)–C–N(4)		122.07(12)	125.11(5)	125.04(10)	124.65(55)	126.7(11)	123.5(3)	126.85(71)
N(1)–Ru–N(3)	–		72.57(13)	73.14(3)	76.12(29)	76.71(3)	72.41(11)	74.05(37)
$\nu(\text{Ru}=\text{C}=\text{O})$ (cm <sup>-1</sup> )			1937	1926	1958	1951	1940	1937

<sup>a</sup>Values from ref 14. <sup>b</sup>Average value given with the difference between the two values for the two independent molecules given in parentheses.

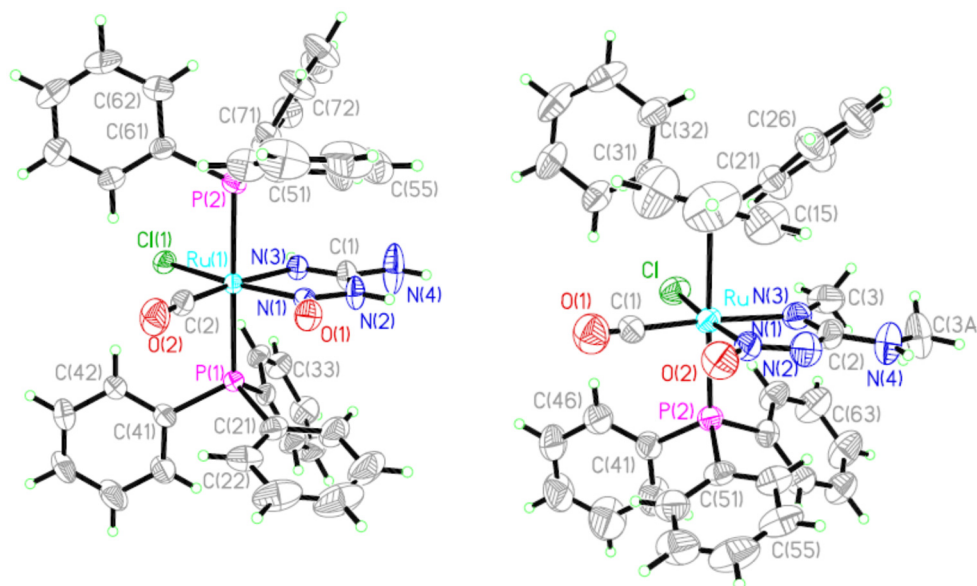


Figure 5. ORTEP representations for the crystal structures of chloride complexes 3a (left) and 3b (right). Note that for 3b the methyl group is equally disordered over two positions [N(3) and N(4)].

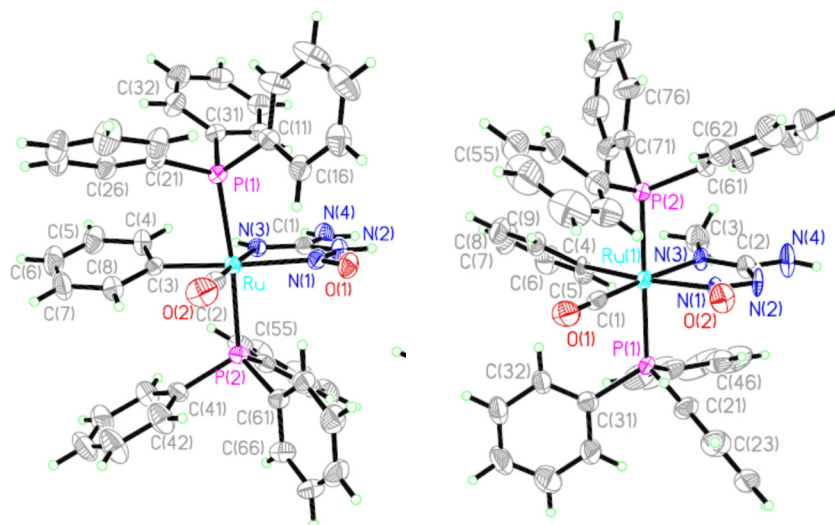


Figure 6. ORTEP representations of phenyl derivatives 4a (left) and 4b (right).

the phenyl and hydride complexes. There is considerable potential for other examples of this class to be discovered. Moreover, there is likely considerable potential coordination sphere reactivity to be discovered for these guanidinyll derivatives.

## ■ ASSOCIATED CONTENT

### Supporting Information

The Supporting Information is available free of charge at <https://pubs.acs.org/doi/10.1021/acs.inorgchem.1c00844>.

Tables of crystallographic, theoretical, and spectroscopy data and figures showing the packing of methylnitroso-guanidine (PDF)

### Accession Codes

CCDC 1969098–1969102, 1999797, and 2005539 contain the supplementary crystallographic data for this paper. These data can be obtained free of charge via [www.ccdc.cam.ac.uk/data\\_request/cif](http://www.ccdc.cam.ac.uk/data_request/cif), or by emailing [data\\_request@ccdc.cam.ac.uk](mailto:data_request@ccdc.cam.ac.uk), or by contacting The Cambridge Crystallographic Data Centre, 12 Union Road, Cambridge CB2 1EZ, UK; fax: +44 1223 336033.

## ■ AUTHOR INFORMATION

### Corresponding Author

D. Scott Bohle – Department of Chemistry, McGill University, Montreal H3A 0B8, Canada; [orcid.org/0000-0001-5833-5696](https://orcid.org/0000-0001-5833-5696); Email: [Scott.Bohle@McGill.ca](mailto:Scott.Bohle@McGill.ca)

### Authors

Mimi Simmons – Department of Chemistry, McGill University, Montreal H3A 0B8, Canada

Kayla Cummings Premack – Department of Chemistry, McGill University, Montreal H3A 0B8, Canada

E. Danae Guerra – Department of Chemistry, McGill University, Montreal H3A 0B8, Canada

Maeve J. Bohle – Department of Chemistry, McGill University, Montreal H3A 0B8, Canada

Kristopher A. Rosadiuk – Department of Chemistry, McGill University, Montreal H3A 0B8, Canada

Complete contact information is available at:

<https://pubs.acs.org/doi/10.1021/acs.inorgchem.1c00844>

### Notes

The authors declare no competing financial interest.

## ■ ACKNOWLEDGMENTS

The authors gratefully acknowledge support of this research from NSERC and the CRC.

## ■ REFERENCES

(1) Muller, A. L.; Bleith, T.; Roth, T.; Wade, H.; Gade, L. H. Iridium Half-Sandwich Complexes with Di- and Tridentate Bis-(pyridylimino)isindolato Ligands: Stoichiometric and Catalytic Reactivity. *Organometallics* **2015**, *34*, 2326.

(2) Cowley, A. R.; Dilworth, J. R.; Donnelly, P. S.; Ross, S. J. Rhenium diazenide ternary complexes with dithiocarbamate ligands: towards new rhenium radiopharmaceuticals. *Dalton Trans.* **2007**, 73–82.

(3) Broere, D. L. J.; Mercado, B. Q.; Lukens, J. T.; Vilbert, A. C.; Banerjee, G.; Lant, H. M. C.; Lee, S. H.; Bill, E.; Sproules, S.; Lancaster, K. M.; Holland, P. L. Reversible Ligand-Centered Reduction in Low-Coordinate Iron Formazanate Complexes. *Chem. - Eur. J.* **2018**, *24*, 9417–9425.

(4) Chakraborty, I.; Panda, B. K.; Gangopadhyay, J.; Chakravorty, A. Rhenium Chemistry of Azooximes: Oxygen Atom Transfer, Azooxime Chelation, and Imine-Oxime Contrast. *Inorg. Chem.* **2005**, *44*, 1054–1060.

(5) Hirsch-Kuchma, M.; Nicholson, T.; Davison, A.; Davis, W. M.; Jones, A. G. The synthesis and characterization of technetium and rhenium hydrazinopyrimidine chelate complexes. *J. Chem. Soc., Dalton Trans.* **1997**, 3185–3188.

(6) Hirsch-Kuchma, M.; Nicholson, T.; Davison, A.; Davis, W. M.; Jones, A. G. Synthesis and Characterization of Rhenium(III) and Technetium(III) Organohydrazide Chelate Complexes. Reactions of 2-Hydrazinopyridine with Complexes of Rhenium and Technetium. *Inorg. Chem.* **1997**, *36*, 3237–3241.

(7) Abrams, M. J.; Larsen, S. K.; Zubieta, J. Synthesis and crystal and molecular structure of a technetium-hydralazino complex. *Inorg. Chim. Acta* **1990**, *173*, 133–135.

(8) Abrams, M. J.; Larsen, S. K.; Shaikh, S. N.; Zubieta, J. Investigations of technetium-organohydrazine coordination chemistry. *Inorg. Chim. Acta* **1991**, *185*, 7–15.

(9) Perez-Lourido, P.; Romero, J.; Garcia-Vazquez, J. A.; Sousa, A.; Maresca, K. P.; Zubieta, J. Synthesis and Characterization of Rhenium(III) Organohydrazide Compounds. Crystal and Molecular Structures. *Inorg. Chem.* **1999**, *38*, 1511–1519.

(10) Danac, R.; Pui, A.; Corja, I.; Amarandi, R.-M.; Ciobanu, C. I.; Apostu, M.-O.; Palamarcu, O. New M(II) (M = Mn, Co, Ni, Cu, Zn, Pd) coordinative compounds with 2-formylpyridine S-methylisothiosemicarbazide. *J. Mol. Struct.* **2020**, *1207*, 127747–127752.

(11) Palii, S. P.; Simonov, Y. A.; Bourosh, P. N.; Gerbeleu, N. V.; Dvorkin, A. A. Template synthesis and study of isomeric nickel(II) coordination compounds with tetradentate ligands based on o-aminobenzaldehyde and S-alkylisothiosemicarbazides. *Koord. Khim.* **1996**, *22*, 129–138.

(12) Nicholson, T.; Cook, J.; Davison, A.; Rose, D. J.; Maresca, K. P.; Zubieta, J. A.; Jones, A. G. The synthesis and characterization of [diazenedo] from [MO<sub>4</sub>]<sup>−</sup> (where M = Re, Tc) organodiazenedo, organodiazene-chelate complexes. *Inorg. Chim. Acta* **1996**, *252*, 421–426.

(13) Nicholson, T.; Zubieta, J. Complexes of rhenium with benzoylazo and related ligands. *Polyhedron* **1988**, *7*, 171–185.

(14) Murmann, R. K.; Glaser, R.; Barnes, C. L. Structures of nitroso- and nitroguanidine x-ray crystallography and computational analysis. *J. Chem. Crystallogr.* **2005**, *35*, 317–325.

(15) Murmann, R. K.; Glaser, R.; Barnes, C. L. Structure of the nitrosoguanidine complexes of nickel(II) and copper(II) by X-ray crystallography and computational analysis. *J. Coord. Chem.* **2005**, *58*, 279–294.

(16) Malatesta, L.; Monica, G. L.; Manassero, M.; Sansoni, M. Further investigations on the oxidation reaction derivatives of bisbenzamidoximatonickel(II). *Gazz. Chim. Ital.* **1980**, *110*, 113–121.

(17) Bikbaeva, Z. M.; Ivanov, D. M.; Novikov, A. S.; Ananyev, I. V.; Bokach, N. A.; Kukushkin, V. Y. Electrophilic-Nucleophilic Dualism of Nickel(II) toward Ni···I Noncovalent Interactions: Semicoordination of Iodine Centers via Electron Belt and Halogen Bonding via  $\sigma$ -Hole. *Inorg. Chem.* **2017**, *56*, 13562–13578.

(18) Bikbaeva, Z. M.; Novikov, A. S.; Suslonov, V. V.; Bokach, N. A.; Kukushkin, V. Y. Metal-mediated reactions between dialkylcyanamides and acetamidoxime generate unusual (nitrosoguanidinate)nickel(II) complexes. *Dalton Trans.* **2017**, 46, 10090–10101.

(19) Tskhovrebov, A. G.; Vasileva, A. A.; Goddard, R.; Riedel, T.; Dyson, P. J.; Mikhaylov, V. N.; Serebryanskaya, T. V.; Sorokoumov, V. N.; Haukka, M. Palladium(II)-Stabilized Pyridine-2-Diazotates: Synthesis, Structural Characterization, and Cytotoxicity Studies. *Inorg. Chem.* **2018**, *57*, 930–934.

(20) Novikov, A. S.; Ivanov, D. M.; Bikbaeva, Z. M.; Bokach, N. A.; Kukushkin, V. Y. Noncovalent interactions involving iodofluorobenzenes: *Cryst. Growth Des.* **2018**, *18*, 7641–7654.

(21) Thiele, J. I. Uber Nitrosoguanidin. *J.v. Liebigs Ann. Chem.* **1893**, *273*, 133–144.

- (22) Efimenko, Z. M.; Eliseeva, A. A.; Ivanov, D. M.; Galmes, B.; Frontera, A.; Bokach, N. A.; Kukushkin, V. Y. Bifurcated  $\mu_2$ -I $\cdots$ (N,O) Halogen Bonding: The Case of (Nitrosoguanidinate)NiII Cocrystals with Iodine(I)-Based  $\sigma$ -Hole Donors. *Cryst. Growth Des.* **2021**, *21*, 588–596.
- (23) Thiele, J.; Dent, F. Ueber nitrosocarbamates. *Liebigs Ann. Chem.* **1898**, *302*, 245.
- (24) Thakkalapally, A.; Benin, V. Synthesis, structural studies and desilylation reactions of some N-2-(trimethylsilyl)ethyl-N-nitrosocarbamates. *Tetrahedron* **2005**, *61*, 4939–4948.
- (25) Benin, V. Secondary N-nitrosocarbamate anions: Structure and alkylation reactions. A DFT study. *J. Mol. Struct.: THEOCHEM* **2006**, *764*, 21–31.
- (26) Venkata, S.; Shamo, E.; Benin, V. Preparation and characterization of some substituted benzyl N-nitrosocarbamates containing an N-2-(methylthio)ethyl or a bis(2-aminoethyl)sulfide functionality. *Synth. Commun.* **2009**, *39*, 1406–1414.
- (27) Tsujiuchi, T.; Tsutsumi, M.; Konishi, Y. Molecular aspects during multi-step chemical induced carcinogenesis in the lung and pancreas. *J. Toxicol. Pathol.* **2003**, *16*, 133–138.
- (28) Hoffmann, D.; Adams, J. D.; Brunemann, K. D.; Hecht, S. S. Formation, occurrence, and carcinogenicity of N-nitrosamines in tobacco products. *ACS Symp. Ser.* **1981**, *174*, 247–273.
- (29) Bohle, D. S.; Chua, Z. Iridium(I) Complexes of  $\pi$ -Acidic Carboxamides. *Organometallics* **2015**, *34*, 1074–1084.
- (30) Bohle, D. S.; Chua, Z.; Perepichka, I.; Rosadiuk, K. Lewis acid stabilization and activation of primary N-nitrosamides. *RSC Adv.* **2017**, *7*, 8205–8219.
- (31) McKay, A. F. Nitroguanidines. *Chem. Rev. (Washington, DC, U.S.)* **1952**, *51*, 301–346.
- (32) Savitt, J. Some Properties and Uses of Nitroguanidine. *Int. Jahrestag Fraunhofer Inst.* **1985**, *16*, 38/31–38/14.
- (33) Thiele, J.; Lachman, A. I. Ueber Nitroharstoff, Nitrourethan und Nitramid. *Liebigs Ann.* **1895**, *288*, 267–311.
- (34) Collins, T. J.; Grundy, K. R.; Roper, W. R. The tris-(triphenylphosphine)osmium zerovalent complexes Os(CO)<sub>2</sub>(PPh<sub>3</sub>)<sub>3</sub>, Os(CO)(CNR)(PPh<sub>3</sub>)<sub>3</sub>, Os(CO)(CS)(PPh<sub>3</sub>)<sub>3</sub>, Os(CS)(CNR)(PPh<sub>3</sub>)<sub>3</sub> and derived compounds. *J. Organomet. Chem.* **1982**, *231*, 161–172.
- (35) Roper, W. R.; Wright, L. J. Ruthenium aryl complexes. *J. Organomet. Chem.* **1977**, *142*, C1–C5.
- (36) Bohle, D. S.; Clark, G. R.; Rickard, C. E. F.; Roper, W. R.; Wright, L. J. Stable terminal methylene complexes of osmium(II) and ruthenium(II). The unexpected preferential migration of a  $\sigma$ -aryl ligand to carbon monoxide rather than to methylene. *J. Organomet. Chem.* **1988**, *358*, 411–447.
- (37) Cavit, B. E.; Grundy, K. R.; Roper, W. R. Ru(CO)<sub>2</sub>(PPh<sub>3</sub>)<sub>3</sub> and Os(CO)<sub>2</sub>(PPh<sub>3</sub>)<sub>2</sub>. An ethylene complex of ruthenium and a dioxygen complex of osmium. *J. Chem. Soc., Chem. Commun.* **1972**, 60–61.
- (38) Davis, T. L.; Rosenquist, E. N. Studies in the Urea Series. XV. Transformations of nitrosoguanidine. Alkynitrosoguanidines. N-R, N'R'-Dialkylguanidines. *J. Am. Chem. Soc.* **1937**, *59*, 2112–2115.
- (39) Benin, V.; Kaszynski, P.; Radziszewski, J. G. Ambident Ethyl N-Nitrosocarbamate Anion: Experimental and Computational Studies of Alkylation and Thermal Stability. *J. Am. Chem. Soc.* **2002**, *124*, 14115–14126.
- (40) Peterson, K. A.; Figgen, D.; Dolg, M.; Stoll, H. Effective Core Potentials. *J. Chem. Phys.* **2007**, *126*, 124101.
- (41) Sheldrick, G. A short history of SHELX. *Acta Crystallogr., Sect. A: Found. Crystallogr.* **2008**, *A64*, 112–122.
- (42) Sheldrick, G. M. *SADABS, TWINABS*; 1996.
- (43) Sabetta, V. J.; Himmelfarb, D.; Smith, G. B. L. Reduction of nitroguanidine. II. Preparation and properties of nitrosoguanidine. *J. Am. Chem. Soc.* **1935**, *57*, 2478–2479.
- (44) Kerone, E. B. W. (Western Cartridge Co.) Nitrosoguanidine from nitroguanidine. US 2146188, 1939.
- (45) Thiele, J. Ueber Nitro- and Amidoguanidin. *Justus Liebigs Ann. Chem.* **1892**, *270*, 1–63.
- (46) Devries, J. I.; Gantz, E. S. C. Spectrophotometric Studies of Dissociation Constants of Nitroguanidines, Triazoles, and Tetrazoles. *J. Am. Chem. Soc.* **1954**, *76*, 1008–1010.
- (47) Hahn, C.; Pribyl, E.; Lieber, E.; Caldwell, B. P.; Smith, G. B. L. Reduction of nitroguanidine. XII. Oxidation potentials of the nitro-nitrosoguanidine and the nitroso-aminoguanidine systems. *J. Am. Chem. Soc.* **1944**, *66*, 1223–1226.
- (48) Spreter, V. C.; Briner, E. The electrolytic reduction of nitroguanidine to aminoguanidine and of nitrourea to semicarbazide-influence of the cathode. *Helv. Chim. Acta* **1949**, *32*, 215–232.
- (49) Mislow, K.; Siegel, J. Stereoisomerism and local chirality. *J. Am. Chem. Soc.* **1984**, *106*, 3319–3328.